RAPID FABRICATION OF MULTIFUNCTIONAL MICROCAPILLARY FOR FOUR-DIMENSIONAL SINGLE CELL MANIPULATION

Yu Ting Chow[1], Tianxing Man[1], Giovanny F. Acosta-Vélez[2], Xiongfeng Zhu[1], Ximiao Wen[1], Pei-Shan Chung[1], Tingyi "Leo" Liu[1], Benjamin M. Wu[2, 3], and Pei-Yu Chiou[1]

[1]Mechanical and Aerospace Engineering Department, University of California, Los Angeles, USA.
[2]Bioengineering Department, University of California, Los Angeles, USA.
[3]School of Dentistry, University of California, Los Angeles, USA.

ABSTRACT

We report a novel manufacturing approach to fabricate liquid metal–based, multifunctional microcapillary pipettes able to provide electrodes with high electrical conductivity for high frequency electrical stimulation and measurement. Four-dimensional single cell manipulation has been realized by applying multi-frequency, multi-amplitude, and multi-phase electrical signals to the microelectrodes near the pipette tip to create a 3D dielectrophoretic trap and 1D electrorotation simultaneously. Functions such as single cell trapping, transferring, patterning, and rotation have been accomplished. Cell viability and multi-day proliferation characterization has confirmed the biocompatibility of this approach. This is a simple, low cost, and fast fabrication approach that requires no cleanroom and photolithography to manufacture 3D microelectrodes and microchannels accessible to a wide user base for broad applications.

INTRODUCTION

Rapid progresses in micro and nano manufacturing have resulted in the advancement in numerous research and application fields in the past few decades. Conventional micro and nano manufacturing methods have several fundamental limitations. They are mainly two-dimensional patterning techniques with limited control in the third dimension. They are also planar techniques that cannot pattern features on non-planar surfaces. Glass micropipette pulling techniques have their unique niche and are widely used in various fields for broad applications, especially in biology, despite the rapid progresses of micro and nano fabrication.[1]–[4] Multifunctional micropipettes can be accomplished by jointly pulling glass capillaries with other materials such as carbon fibers, or metal nanoparticles.[5] However, the electrical properties, such as the electrical conductivity of the pulled wires, are not easy to control, and the post-processing of the composite pipettes before they can be used could be complicated.[6], [7]

Here, we demonstrated a liquid metal-filled multifunctional microcapillary pipette that is easy to fabricate and can provide electrodes with high electrical conductivity for high frequency measurement and excitation. The glass capillary is heated and pulled with a micropipette puller. The pulled capillary is then filled with gallium through a syringe. Centrifuge is used to push the gallium to the needle tip. To demonstrate a potential application, the fabricated multi-barrel and multi-electrode pipettes are used to provide 3D DEP trap and 1D electrorotation simultaneously.

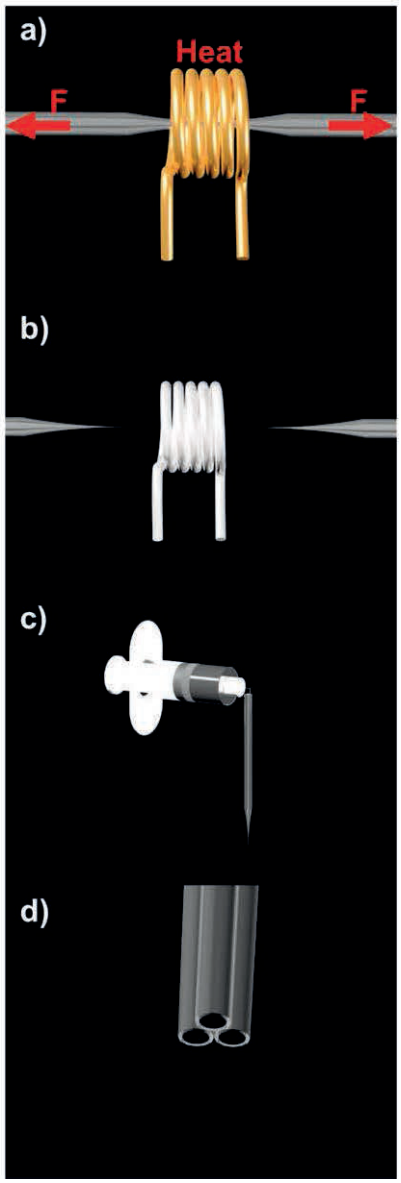

Figure 1: Fabrication process of liquid metal filled multifunctional micropipette. a) A multi-barrel glass capillary is heated and b) pulled with a custom-made micropipette puller. c) The micropipette is then filled with liquid gallium using a syringe and centrifuge to drive the gallium to the tip. After that, the micropipette is trimmed by a custom-made microforge to have a desired tip diameter. d) The final product.

METHODOLOGY

Fabrication of the Liquid Metal-based Microcapillary

The fabrication process of a multi-barrel, liquid metal

filled pipette is shown in Fig. 1. It starts from heating and pulling a multi-barrel glass pipette with a custom-made puller. Liquid gallium is then filled in selected barrels through a syringe. A centrifuge is used to spin and push liquid gallium all the way to the tip. A custom-made microforge is used in the last step to trim the tip. Comparing to conventional microfabrication, the proposed approach does not require any cleanroom and photolithography processes to create these long, patterned, three-dimensional microelectrodes. This can save the manufacturing cost, speed up the design process, and allow rapid adjustment of electrode sizes for different applications. As a demonstration of this new fabrication method, 3- and 7-barrel micropipettes are fabricated as shown in Fig. 2. The measured electrical resistance of a cm-long, tapered liquid metal electrode with a 7 μm opening tip is 12 to 15 Ω. This low electrical resistance of the fabricated electrode permits high frequency electrical excitation and measurement near the micropipette tip without losing power in the long electrical conduction wire. In this paper, a 3-barrel micropipette is further used to perform 4D single cell manipulation by simultaneously applying a 10 MHz electrical signal to create a 3D dielectrophoretic cell trap, and a 400 kHz signal to induce electrorotation on the trapped cell.

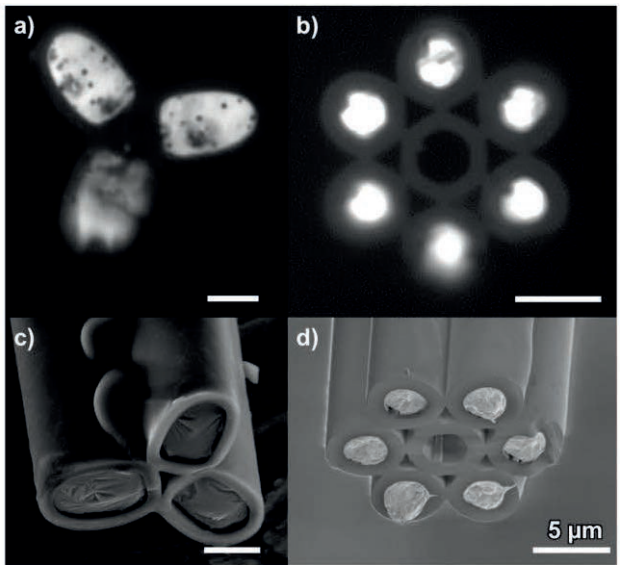

Figure 2: a) and b) Microscopic images of the pulled multibarrel micropipettes selectively filled with liquid metal in desired channels. The center channel of the 7-barrel pipette is kept empty to allow fluid delivery. c) and d) Scanning electron microscopic (SEM) images of the micropipettes.

Working Principle of Dielectrophoresis (DEP)

DEP is a phenomenon in which a particle in a non-uniform electric field is polarized and interacts with the applied field to generate a net force moving the particle towards a strong electric field region if it is more polarizable than the medium (positive DEP), or to a weak field region if the particle is less polarizable than the medium (negative DEP). The time-averaged DEP force on a particle in a non-uniform electric field (E-field) is given by the following equation.[8]

$$< \mathbf{F_{DEP}} >= 2\pi \mathbf{r^3}\, \epsilon_m\, \mathbf{Re}\left(\frac{\epsilon_p^* - \epsilon_m^*}{\epsilon_p^* + 2\epsilon_m^*}\right) \nabla \mathbf{E^2}$$

where r is the radius of the particle, ϵ_m is the permittivity of the medium, **E** is the E-field, and $\mathbf{Re}(\frac{\epsilon_p^* - \epsilon_m^*}{\epsilon_p^* + 2\epsilon_m^*})$ is the real part of the Clausius-Mossotti (CM) factor. ϵ_p^* and ϵ_m^* are the complex permittivity of the particle and medium respectively. The magnitude of DEP force depends on the gradient, the frequency, and the amplitude of the E-field, and the size of the particle. DEP has been widely used for cell manipulation in the past decade for cell trapping and sorting applications. DEP manipulation of biological cells in aqueous media is typically carried out with electrical signals in a frequency range between 100 kHz and 10 MHz. Within this frequency range, cell viability can be maintained, and different types of cells show significantly different dielectric properties.

The schematic of a 3-barrel pipette DEP tweezers is shown in Fig. 3a. Gallium is filled in all three channels to form electrodes. AC electrical signals are applied to these three gallium electrodes for creating a non-uniform electric field distribution to induce DEP forces on nearby objects. If a positive DEP force is induced on a cell nearby, it will be attracted to the strong electric field region near the center of the pipette tip.

Working Principle of Electrorotation (ROT)

ROT is a phenomenon in which a particle rotates in a rotating electric field. It is the result of the phase delay between the induced electric dipole on the particle and the external rotating field. This delay creates an angel between the directions of the induced dipole and the external field, which results in a mechanical torque rotating the particle. What determines the direction and the magnitude of the torque on a particle are the electric field strength, frequency, and the dielectric composition of particles.

DEP and ROT have a similar physical origin, both based on the interactions between the field-induced dipole on a particle and the external field. Based on cells' dielectric signatures, both DEP and ROT have been shown to be able to provide label-free characterization of different types of cells[9], [10] or cells at different growth phases.[11]

The 3-barrel micropipette shown in Fig. 2b can also be utilized to rotate the trap cell in the axial direction by applying 120^0 phase difference AC signals to the three electrodes (Fig. 3). The electrorotation torque **Γ** is given by the following equation.[8]

$$< \mathbf{\Gamma} >= -4\pi \mathbf{r^3} \epsilon_m \mathbf{Im}\left(\frac{\epsilon_p^* - \epsilon_m^*}{(\epsilon_p^* + 2\epsilon_m^*)}\right) |\mathbf{E}|^2$$

where $\mathbf{Im}(\mathbf{f_{cm}})$ is the imaginary part of the CM factor.

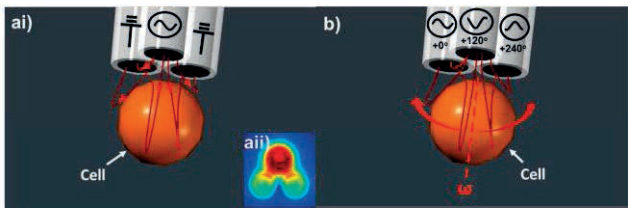

Figure 3: The schematic of using a multi-barrel liquid metal pipette for DEP trap and electrorotation. ai) DEP force is generated by applying AC signals to the three electrodes. aii) The electric field distribution near the pipette tip. b) Three AC signals with 0, 120^0, and 240^0 phase differences are applied to the three electrodes to create rotating fields.

RESULTS

DEP Force Calibration

The DEP force is hard to measured directly by measuring the E-field strength and distribution near the tip. Instead, the velocity of the cell just before it touches the tweezers can be used to compute the DEP force, since the magnitude of the drag force experienced by the cell is equal to that of the DEP force. The drag force of a spherical particle is given by Stokes' equation[12].

$$\boldsymbol{F_{Drag} = 6\pi r v \eta}$$

where $\boldsymbol{\eta}$ is the dynamic viscosity of the medium, $\boldsymbol{v}$ is the velocity of the particle and $\boldsymbol{r}$ is the radius of the particle. In this paper, the dynamic viscosity of the medium is assumed to be equal to 10^{-3} Pa.s and the diameter of the Hela cell is about 20 µm. In the isotonic buffer, the live Hela cell experiences positive DEP force while the dead Hela cell experience negative DEP force. The force measurement results are shown in Fig. 4. From Fig. 4a, the DEP force experienced by the cell as a function of distance to the tip is shown. Since the E-field near the tip is highly non-uniform, only the cell near the tip will get trapped. Hence, this electrode configuration is good for single cell manipulation. From Fig. 4b, the DEP force has a strong quadratic dependence with the voltage applied.

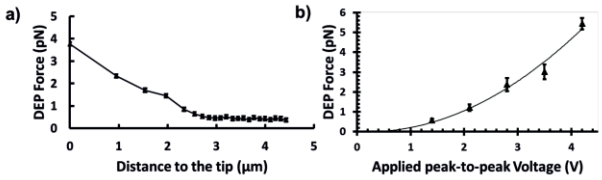

Figure 4: DEP force calibration. a) The DEP force was determined by measuring the velocity of the cell before it touched the tip (0 µm). A 10 MHz, 2.8 V_{pp} AC signal is applied. b) A plot of the maximum DEP force against the applied peak-to-peak voltage.

Cell Manipulation and Electrorotation

To demonstrate the potential applications, a 3-barrel pipette with all channels filled with liquid metal electrodes is used for four-dimensional single cell manipulation. By applying multi-phase, multi-amplitude, multi-frequency AC signals to the micropipette to create 3D DEP trap and 1D electrorotation, functions such as single cell trapping, transferring, patterning, and rotation can be accomplished.

Fig. 5 shows a 'AL' cell pattern formed by sequentially trapping, transferring, and releasing of single cells. One very unique feature of this pipette is that by applying AC signals with 0, 120^0, 240^0 phase differences to the three electrodes, electrorotation can be induced to rotate the trapped cell in the axial direction of the pipette, as shown in Fig. 5b. Note that, all the experiments are done on a regular Petri dish. No additional electrodes are required during the manipulation process. The multifunctional pipette contains all the necessary electrodes for the 4D cell manipulation.

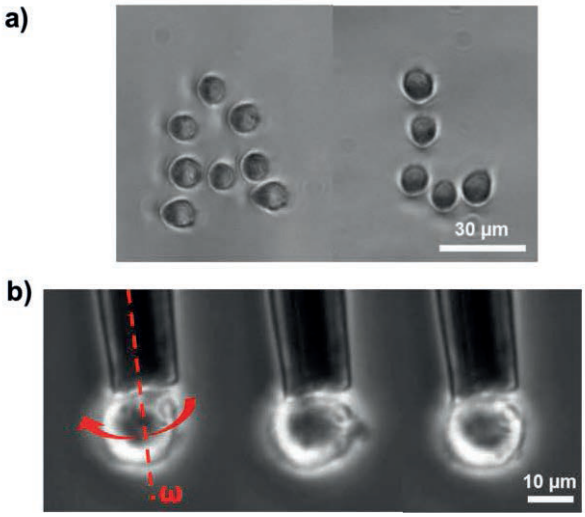

Figure 5: Cell manipulation results. a) A "AL" pattern was formed by using the micropipette to trap, transfer, and unload single cells. A 10 MHz, 1.6 V_{pp} AC signal is applied to the micropipette. Ramos B cell was used in this experiment. b) A trapped cell near the tip was rotated by applying 3.2 V_{pp} and 400 kHz AC signals with 0, 120^0, phase differences to the three electrodes. PANC-1 cell was used in this experiment. Red dotted line is the cell rotation axis.

Cell Viability Test

Cell viability test was conducted to investigate the potential impacts on cells after manipulation. The cell viability was evaluated 12 hours after the DEP manipulation. The cell viability is defined as the number of calcein AM positive cells over the number of cells in the microwell right after DEP manipulation. In addition, the multi-day proliferation rate of the manipulated cells was tracked for 3 days. At day 3, the cells were stained with calcein AM to count the number of live cells. The proliferation rate is defined as the total number of cells (including dead cells) after 3 days over the number of cells in the same microwell right after DEP manipulation. In Fig. 6a and 6b, cell viability is > 90% in all cases and the proliferation rate is > 180% for all applied voltage.

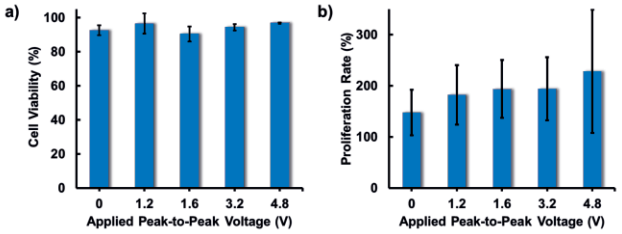

Figure 6: Cell viability analysis. a) The cell viability test was conducted 12 hours after the DEP manipulation at different voltages. b) The cell proliferation rate 3 days after the DEP manipulation at different voltages. Hela cells are used in this study.

CONCLUSION

In conclusion, we demonstrate a liquid metal–based, multifunctional microcapillary pipettes able to provide electrodes with high electrical conductivity for high frequency electrical stimulation and measurement. This technique has various advantages. First, the selective gallium filling of individual channel enables the integration of microfluidics and electrodes. Second, the tip size of the tweezers can be adjusted for manipulating cells of different sizes without redesigning a mask. Third, this technique does not rely on cleanroom equipment which makes it easily assessable to broad users. To demonstrate the potential use of this novel fabrication method, a 3-barrel glass capillary filled with gallium is shown to have the capability to perform four-dimensional single cell manipulation, 3D DEP trapping and 1D electrorotation with high cell viability.

ACKNOWLEDGEMENTS

This work is supported by NSF ECCS 1711507 and NIH R01NX087494.

REFERENCES

[1] Y. T. Chow *et al.*, “A High-Throughput Automated Microinjection System for Human Cells with Small Size,” *IEEEASME Trans. Mechatron.*, vol. 21, no. 2, pp. 838–850, Apr. 2016.

[2] Y. T. Chow *et al.*, “Single Cell Transfection through Precise Microinjection with Quantitatively Controlled Injection Volumes,” *Sci. Rep.*, vol. 6, p. 24127, Apr. 2016.

[3] C. Chen and A. Folch, “A high-performance elastomeric patch clamp chip,” *Lab Chip*, vol. 6, no. 10, pp. 1338–1345, 2006.

[4] D. Franz, H. L. Olsen, O. Klink, and J. Gimsa, “Automated and Manual Patch Clamp Data of Human Induced Pluripotent Stem Cell-Derived Dopaminergic Neurons,” *Sci. Data*, vol. 4, p. 170056, 2017.

[5] A. Piironen, M. Weckström, and M. Vähäsöyrinki, “Ultrasmall and Customizable Multichannel Electrodes for Extracellular Recordings,” *J. Neurophysiol.*, vol. 105, no. 3, pp. 1416–1421, Mar. 2011.

[6] A. Gumennik *et al.*, “Silicon-in-Silica Spheres Via Axial Thermal Gradient in-Fibre Capillary Instabilities,” *Nat. Commun.*, vol. 4, p. ncomms3216, Jul. 2013.

[7] J. J. Kaufman *et al.*, “Structured Spheres Generated by an in-Fibre Fluid Instability,” *Nature*, vol. 487, no. 7408, pp. 463–467, Jul. 2012.

[8] T. B. Jones, “Basic Theory of Dielectrophoresis And Electrorotation,” *IEEE Eng. Med. Biol. Mag.*, vol. 22, no. 6, pp. 33–42, Nov. 2003.

[9] U. Kim, J. Qian, S. A. Kenrick, P. S. Daugherty, and H. T. Soh, “Multitarget Dielectrophoresis Activated Cell Sorter,” *Anal. Chem.*, vol. 80, no. 22, pp. 8656–8661, Nov. 2008.

[10] R. Hölzel, “Non-Invasive Determination of Bacterial Single Cell Properties by Electrorotation,” *Biochim. Biophys. Acta BBA - Mol. Cell Res.*, vol. 1450, no. 1, pp. 53–60, May 1999.

[11] U. Kim, C.-W. Shu, K. Y. Dane, P. S. Daugherty, J. Y. J. Wang, and H. T. Soh, “Selection of Mammalian Cells Based on Their Cell-Cycle Phase Using Dielectrophoresis,” *Proc. Natl. Acad. Sci.*, vol. 104, no. 52, pp. 20708–20712, Dec. 2007.

[12] H. Bruus, *Theoretical microfluidics*. Oxford ; New York: Oxford University Press, 2008.

CONTACT

1. Yu Ting Chow, tel: +1-310-825-7457; yutchow@ucla.edu
2. Pei-Yu Chiou, tel: +1-310-825-8620; pychiou@gmail.com